Casting Solutions for Readiness

Thin Wall and High Strength Die Casting Alloys

September 17, 2017

R. Allen Miller

Professor Emeritus, The Ohio State University

Abstract

Fluidity for casting is defined as the distance that the metal will flow before the onset of solidification stops continued flow. Fluidity is clearly an important issue when determining if a casting, particularly a thin walled casting, will fill. While both the properties of the cast alloy and the processing conditions impact the fluidity of the alloy, it is less clear what the relative contribution of the material, process, and the part itself are to the ability to fill the die cavity. A relatively simple one-dimensional heat transfer model that incorporates part wall thickness, injection and die temperatures, gate speed plus the freezing range and fraction solid curve of the alloy was developed to analyze this question. Determination of the gate area needed to successfully fill the die cavity at the minimum acceptable metal speed while maintaining an acceptable metal state at the end of fill was an unexpected benefit derived from this model.

The basic fluidity model was extended to incorporate varying speed and/or wall thickness. This extension enables analysis of prefill, or the situation where the cavity is partially filled before the onset of the fast shot or high-speed phase of cavity filling, and provides insight into the conditions under which prefill is beneficial and where it is not likely to be successful.

Several computation factorial experiments were performed using the basic model and analyzed to understand the relative importance of each factor as a contributor to flow distance. The results show that, while the alloy properties do affect the flow distance, flow distance or fluidity is largely a thermal issue controlled by the process conditions. This result provides support for the observation that the casting alloy should be selected to meet the functional requirements of the part without undue consideration of fluidity. The process conditions can then be optimized to produce an acceptable casting.

The fluidity model has been implemented and fully integrated in three web-based applications available on the NADCA Members Plus website. The three applications are:

1) PQ^2
2) Max Flow Time Estimator
3) Gate Designer

The PQ^2 application is used to properly size the in gate to the cavity to meet part quality requirements and to maximize the size of the operating window of the process.

The second of these applications estimates pre-injection heat losses, i.e. losses during ladling, pouring and residence of the metal in the cold chamber prior to injection. This set of calculations replaces a difficult to estimate quantity, the temperature of the metal at the gate, with estimates based on more easily obtained data.

The gate designer application is primarily intended for constructing gate geometries that facilitate metal flow into the cavity but the gate area calculation is included so that users who do not perform a PQ^2 analysis first have access to the result.

The course presentations and text materials used for PQ^2 and Gating have been revised to include the new results. The revised materials have been used for courses taught numerous times starting with the second quarter of 2016.

Introduction and Background

The primary objective of this work was, through modeling, to understand the process and die design factors that limit the ability to fill thin walled castings. Consequently, the focus has been on modelling heat transfer during cavity fill and using the resulting model to perform sensitivity studies that help to explain the relative contribution of key factors including geometry, alloy and process variable on the ability to fill the die cavity. This work has been reported in recent NADCA Transactions (Miller 2015, Miller 2016) and additional details are available in these papers. A third analysis extended the model to include time-varying shot speeds and variable wall thicknesses.

The heat transfer mechanism during cavity filling is distinct from heat transfer post fill and is heavy heavily dependent on convection. Due to the very thin thermal boundary layers involved (see for example (Dantzig and C. L. Tucker 2001)) it is impractical for conventional simulation techniques to resolve the thin layer and accurately capture this phenomena. Simulation models tend to use conduction models instead of convection (i.e. they ignore the mass transfer aspects of the problem) and produce at best a rough approximation of the heat loss during fill.

A simpler, more straight forward, approach is used in this work. The die casting die performs many functions but the one of interest in this work is that of a heat exchanger. The die extracts heat from the moving alloy as it enters the cavity in the same manner that a single pass heat exchanger exchanges heat with a moving fluid. The techniques of heat exchanger design as described in (Lienhard V and Lienhard IV 2011), or any standard heat transfer text, were modified to account for latent heat release, and directly applied to model heat loss during cavity filling. An extremely important step in this approach is the use of a convective heat transfer coefficient obtained from the Nusselt number correlation for liquid metal heat transfer (Reed 1987). The correlation is a power-law type expression that is a function of the hydraulic diameter of the metal flow channel, the mass flow rate of the metal, and standard alloy properties. Consequently, the heat transfer function is a function of the geometry, material and operating conditions.

The roots of this approach trace to a nearly 50 year old paper by Professor Jack Wallace and one of his students (Lindsey and Wallace 1968). Lindsey and Wallace considered heat loss during die filling to be analogous to the operation of a single stream heat exchanger that can be analyzed with the heat exchanger effectiveness method. Heat exchanger terminology was adopted in which the temperature of the material entering the heat exchanger is the temperature at the gate, the heat exchanger wall temperature is the die surface temperature, and the exit temperature is assumed to be the temperature of the metal at the end of fill.

Lindsey and Wallace further assumed that the optimal fill time is such that the metal temperature will be at the liquidus temperature at the end of fill, i.e. solidification does not start until fill is complete. This assumption eliminated the need to consider the complexity of latent heat release but it limited the applicability of the equation since, in general, the casting will be partially solidified at the end of fill and the temperature will be below the liquidus temperature. It was the recognition of the need to account for latent heat that led others to make ad hoc, empirical, adjustments to account for latent heat, e.g. (Herman 1996), but the modified procedure fails to satisfy the principle of conservation of energy and provides a biased estimate of the available cavity fill time (the available time is over estimated).

In this work, heat exchanger results were extended to include the release of latent heat. The resulting model enables estimation of the metal flow time and distance as a function of the alloy material properties, average die cavity wall thickness, and key process parameters. The parameters will be described in detail in the next section. The model provides a vehicle to perform sensitivity analyses that explain the relative contribution of alloy, geometry, and process conditions.

As described previously, fluidity from a casting perspective is defined in terms of the distance that molten metal will flow before solidification reaches the point that flow can no longer be sustained. Flow distance is a function of both process conditions and cast alloy, but the relative contribution of each has never been clear. The process conditions control the rate of heat loss to the die which in combination with the material properties determine the state of the material at any point during filling. Ultimately, the point at which the material will no longer support flow determines the conditions at which flow will stop. The model was used to perform sensitivity analyses based on computational experiments that help to explain the relative contributions of process and material to flow distance or fluidity.

One of the model inputs is a target fraction solid that controls the end of fill condition. If the material state conditions that control stoppage were known, these conditions could be used to calculate the target fraction solid, but these conditions are not known. The traditional models of flow distance are briefly reviewed in order to delineate the differences in the flow conditions that exist in die casting compared to gravity casting. The ratio of kinetic energy to heat is shown to be four orders of magnitude larger in die casting, so much so that dissipation of kinetic energy dominates heat as a stoppage condition. The dimensionless version of the Navier-Stokes equation is used to show that inertial forces dominate viscous forces at the start of fill in die casting, but not in gravity casting. Viscosity increases as the part solidifies and the fraction solid increases. When the viscosity increases sufficiently, viscous forces become relevant and inertia no longer dominates. When viscous forces are sufficiently large, flow will stop. An estimate of the point where viscous forces become relevant can be made using the viscosity curve. An example of this type of analysis is included and it is exactly this type of information that determines the maximum practical fraction solid for an alloy. However, at present this type of analysis is order of magnitude at best and additional work is needed to fully understand the phenomena.

Model Development

A summary of the model development is provided in this section. Additional details of the model development including latent heat analysis are included in an Appendix. Additional details are also included in a NADCA transactions paper (Miller 2015).

Sensible and Latent Heat

Some of the terms used in the maximum flow time model are easier to understand when viewed from the perspective of how the temperature of a typical casting changes with time as the casting alloy cools and solidifies. An approximation of such a curve is shown in Figure 1.

The temperature range over which the alloy solidifies is marked by the alloy's liquidus temperature at the fully liquid end and the solidus temperature at the fully solid end. Superheat is the heat content of the alloy that raises the temperature above the liquidus temperature.

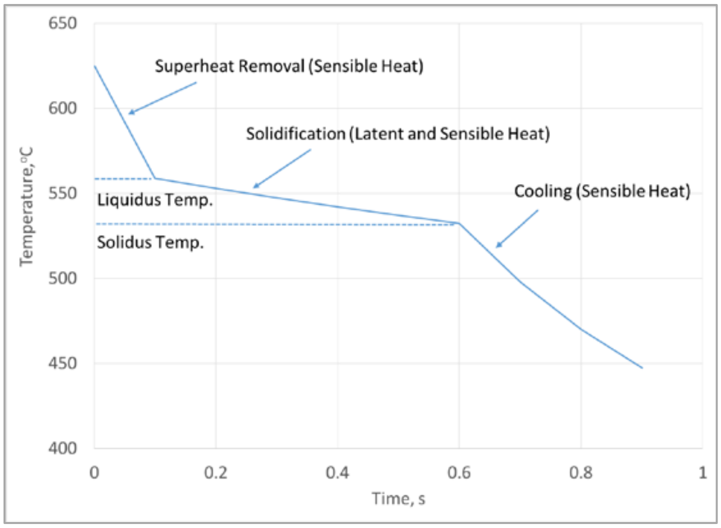

Figure 1 Typical temperature curve for solidifying casting

The rate of change of temperature with time changes significantly at the liquidus and solidus temperatures. The slower drop in temperature during solidification is due to the release of latent heat. Once the solidifying range is reached, the solidifying alloy releases both latent heat and sensible heat. Latent heat is defined as heat that when added or removed does not exhibit a temperature change. The amount of latent heat in the alloy greatly exceeds the sensible heat over the solidifying range in most cases. For example, aluminum 380 has a liquidus temperature of about 1100 ^{o}F (593 ^{o}C), a solidus of about 1000 ^{o}F (538 ^{o}C), and a specific heat of about 0.23 BTU/lb - ^{o}F (0.963 J/g - ^{o}C). Consequently, the sensible heat that is released over the 100 ^{o}F solidifying range is about 23 BTU/lb (53 J/g). The latent heat for 380 is about 167 BTU/lb (388 J/g), about seven times greater.

While the latent heat release doesn't change the alloy temperature during solidification, it is still heat that must be carried away by the die. Therefore, on a per degree basis, much more heat must be transferred to the die per degree of casting temperature change in the solidifying range than in the superheat region or in the fully solidified region. Consequently, the rate of change of the curve in Figure 1 is much lower in the solidifying region than in the superheat and cooling regions.

Fraction Solid

Figure 2 illustrates a linear approximation to a fraction solid versus temperature curve. The fraction solid is equal to 1 (completely solid) at temperatures below the solidus temperature and is equal to zero (completely liquid) at temperatures above the liquidus temperature. In between the fraction solid changes in a nonlinear fashion depending on the alloy, but a linear approximation is reasonable for purposes of determining heat release as a function of temperature for a fluidity analysis. The assumption of a linear curve means that approximate fraction solid is proportional to temperature,

$$f_s(T)=\begin{cases}1 & T\le T_{sol}\\ \dfrac{T_{liq}-T}{T_{liq}-T_{sol}} & T_{sol}<T\le T_{liq}\\ 0 & T_{liq}<T\end{cases} \tag{1}$$

This approximation is used with the gating equation. The heat transfer analysis can be performed using nonlinear fraction solid curves, but the complexity requires computer programs designed for the purpose. Details of the full nonlinear approach can be found in (Miller 2015).

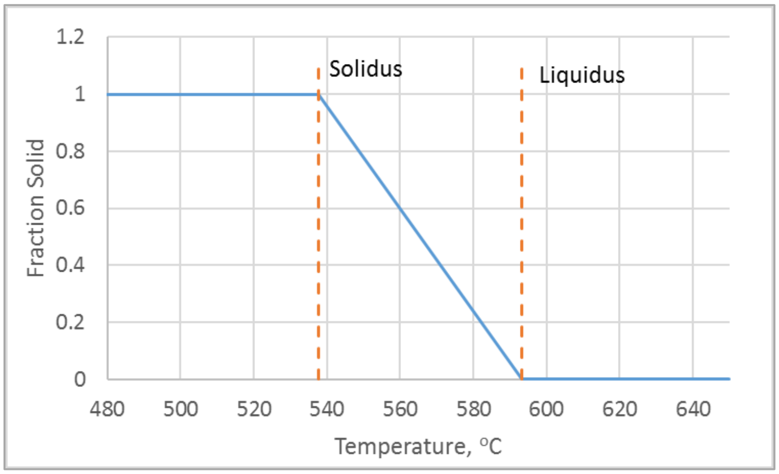

Figure 2 Fraction Solid Curve, Linear Approximation

Heat Transfer Analysis

An acceptable fill time depends on the cavity volume, wall thickness and the distance that the metal must flow to fill the cavity. A heat transfer-based equation for flow time is presented below followed by a description and discussion of the parameters used.

The equations and steps outlined below explain how to calculate three strongly related quantities; flow time t_{f_s}, flow distance x_{f_s}, and the gate area A_g.

- The flow time t_{f_s} is the time from start of cavity filling until the first material entering reaches fraction solid f_s. f_s is a user input selected based on part quality requirements.
- The flow distance x_{f_s} is the distance that the metal flows in the above time interval.
- A_g is the gate area required if the cavity is to be filled in exactly this amount of time, i.e. if t_{f_s} is to be considered the cavity fill time and not just the length of time that the material will flow.

The estimate of flow time and flow distance is based on heat transfer analysis using the model depicted in Figure 3. Details can be found in (Miller 2015). The basic assumptions are that liquid metal is flowing at speed v_g (the gate speed) across the die surface which is at constant temperature T_{die}. The temperature variation of the metal in the y direction is assumed to be small based on the high diffusivity of the alloy so the metal temperature is considered to depend on the *x* position only, i.e. a function of the distance traveled for the short period of time that the die is filling. Temperature as function of distance is denoted by *T(x)*. The analysis is performed on the small slice of width *dx* shown in the figure.

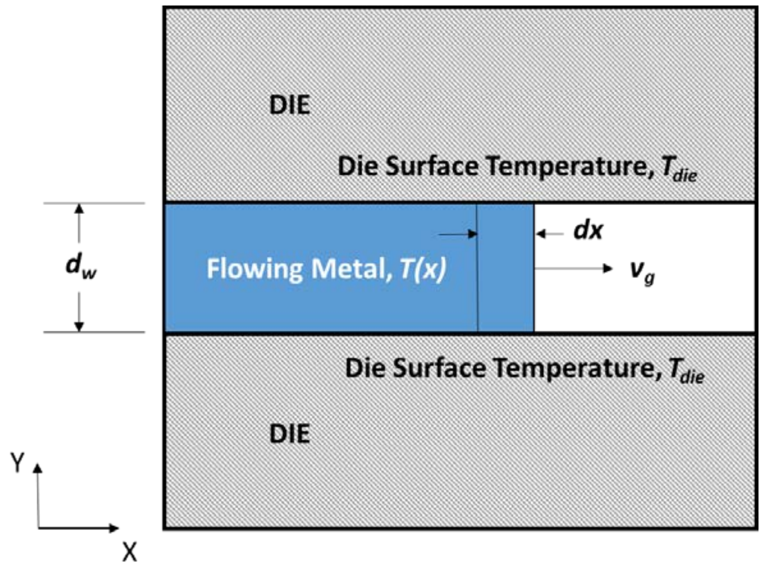

Figure 3 Metal Flow Model

The metal is cooled by convection as it flows across the surface and Newton's law of cooling states that the heat flux is proportional to the difference in temperature of the body and the adjacent wall. The first law of thermodynamics (conservation of energy) states that the rate of change of energy of the body of metal is proportional to the rate of heat transfer into or out of the body. Since the speed is assumed to be constant, the problem can be expressed in terms of distance *x* as well as time since distance is speed multiplied by time.

The Model

As shown in (Miller 2015) analysis of the temperature in the small volume of metal of width *dx* as a function of distance traveled, *x*, at speed v_g leads to the following equations for flow time, flow distance, and gate area:

$$t_{f_s} = \frac{d_w}{2}\frac{\rho \cdot c_p}{h}\left[\begin{array}{l} -\ln\left(\dfrac{T_{liq} - T_{die} - f_s \cdot \left(T_{liq} - T_{sol}\right)}{T_{gate} - T_{die}}\right) \\ -\dfrac{L_f}{c_p \cdot \left(T_{liq} - T_{sol}\right)}\ln\left(\dfrac{T_{liq} - T_{die} - f_s \cdot \left(T_{liq} - T_{sol}\right)}{T_e - T_{die}}\right) \end{array}\right] \tag{2}$$

$$x_{f_s} = v_g \cdot t_{f_s} \tag{3}$$

$$A_g = \frac{V_{cav}}{v_g \cdot t_{f_s}} = \frac{V_{cav}}{x_{f_s}} \tag{4}$$

The gate speed, or the average speed of the metal through the gate, is a required input for the calculations since the heat transfer coefficient depends on the gate speed and because the gate speed and flow time determine flow distance via the standard speed – time - distance relationship.

The parameter definitions, organized by the source or type of data, are summarized in the following table. Additional discussion of key parameters follows the table.

Table 1 Parameters

Property	Description	Units
Alloy Properties		
T_{liq}	Liquidus temperature	^oC (^oF)
T_{sol}	Solidus temperature	^oC (^oF)
ρ	Density	kg/m^3 (lb/in^3)
c_p	Specific heat	J/kg ^oK (BTU/lb ^oF)
L_f	Latent heat of fusion	J/kg (BTU/kg)
k	Thermal conductivity	W/m ^oK (BTU/s in °F)
Cavity and Process Inputs		
V_{cav}	Cavity volume	m^3 (in^3)
v_g	Gate speed, average speed of metal through the gate	m/s (in/s)
f_s	Target fraction solid at end of fill. Must satisfy $0 \le f_s \le 1$	dimensionless
T_{gate}	Temperature of metal at the gate, injection temperature	^oC (^oF)
T_{die}	Average die cavity surface temperature at injection	^oC (^oF)
T_e	Solidification Analysis Start Temperature. Computed variable, see Equation (5).	^oC (^oF)
d_w	Part average wall thickness	m (in)
Heat Transfer Coefficients		
h_{surf}	Surface heat transfer coefficient. Default value: 65,000 W/m^2 ^oK, (0.0221 BTU/s in² °F):	W/m^2 ^oK (BTU/s in² °F)
h_c	Convective heat transfer coefficient. Computed variable, see Equation (9)	W/m^2 ^oK (BTU/s in² °F)
h	Effective heat transfer coefficient. Computed variable, see Equation (6)	W/m^2 ^oK (BTU/s in² °F)
Outputs		

t_{f_s}	Flow time, elapsed time from injection to target fraction solid	s
x_{f_s}	Avg. distance flow front travels (flow distance) at gate speed v_g	m (in)
A_g	Gate area required to meet these conditions	m^2 (in^2)

Solidification Start Temperature T_e

This is a computed parameter used to simplify calculation. As illustrated by Figure 1, the dynamics of the response are different above and below the liquidus temperature and this variable accounts for this fact. The definition is as follows

$$T_e = \begin{cases} T_{liq} & \text{if } T_{gate} > T_{liq} \\ T_{gate} & \text{if } T_{gate} \le T_{liq} \end{cases} \tag{5}$$

The logic is simply that if the gate temperature is above the liquidus temperature, the superheat must first be removed and the solidification portion of the analysis starts at liquidus. If the gate temperature is below the liquidus temperature, solidification started before the metal reached the gate and the solidification phase of this analysis starts at the gate. With this definition, equation (2) correctly accounts for both cases.

Heat Transfer Coefficient

The heat transfer coefficient is the primary empirical parameter in equation (2). During fill, when the metal is moving at a high rate of speed, convection is the most import heat transfer mode and the corresponding heat transfer coefficient is a function of the metal speed and part thickness. Based on experimental results, (Lindsey and Wallace 1968) researchers also hypothesized the presence of a series resistance to heat flow due to oxidation and lube buildup on the die surface as depicted in the simple diagram shown below where the dashed red slice depicts the surface buildup on the interface between the die and part.

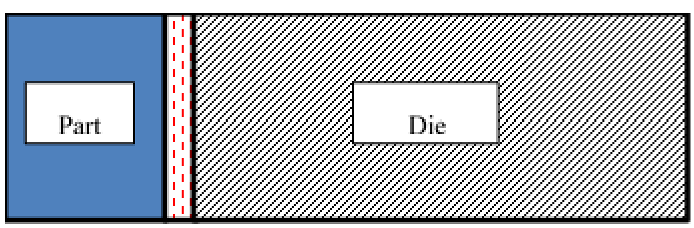

Figure 4 Part – Interface – Die Surface Relationship

The overall resistance R based on this assumption is the sum of the reciprocals of the heat transfer coefficients,

$$R = \frac{1}{h} = \frac{1}{h_{surf}} + \frac{1}{h_c} \tag{6}$$

The overall heat transfer coefficient will be addressed after consideration of each term.

Convective Heat Transfer Coefficient

Dimensional analysis is the standard approach for determining the functional form of convective heat transfer coefficients. Nusselt number correlations based on pipe flow conditions are used as the basis for calculations and the hydraulic diameter applicable to the specific case used to construct an applicable approximation. That is the approach that is taken here.

For most fluids, dimensional analysis finds that the Nusselt number correlation is a function of the Reynolds number and the Prandtl number. However, due to high thermal conductivity, the Prandtl number of liquid metals is very low. At low Prandtl numbers viscosity disappears from the functional equations derived from dimensional analysis and the Nusselt number for both flat plates and tubes is a function only of the Peclet number (Lienhard V and Lienhard IV 2011).

The following dimensionless quantities are used for the analysis. The subscript D in each definition refers to the use of the hydraulic diameter in the calculation:

$$\begin{aligned} D_H &@ \frac{4A_c}{P}; \text{ Hydraulic diameter} \\ Nu_D &@ \frac{h_c D_H}{k}; \text{ Nusselt number} \\ Pe_D &@ \frac{v_m D_H}{\alpha}; \text{ Peclet number} \end{aligned} \tag{7}$$

where:

A_c	Flow cross sectional area, *m^2, (in^2)*
P	Wetted perimeter of flow, *m, (in)*
k	Thermal conductivity, *W/m °K, (BTU/s in °F)*
α	Thermal diffusivity of alloy, *m^2/s, (in^2/s)*
v_m	Average metal speed, *m/s, (in/s)*

The Reed correlation for the Nusselt of liquid metals under constant wall temperature conditions (Reed 1987) is appropriate for this application. See (Reed 1987) and (Kakac, Shah et al. 1987) for additional discussion. The Reed correlation is

$$Nu_D = 3.3 + 0.02 Pe^{0.8}, Pe_D > 100, \frac{x_{f_s}}{D_H} > 60 \tag{8}$$

Using the definition of the Nusselt number and the Peclet number from equation (7), the convective heat transfer coefficient is given by the following power law:

$$h_c = \frac{k}{D_H}\left(3.3 + 0.02 Pe_D^{0.8}\right) = \frac{k}{D_H}\left(3.3 + 0.02\left(\frac{v_m D_H}{\alpha}\right)^{0.8}\right) \tag{9}$$

The hydraulic diameter must be selected according to the flow case under consideration. If the entire perimeter is wetted or two walls are wetted and the hydraulic diameter is approximately twice the average wall thickness.

$$D_H = \frac{4d_w w_w}{2d_w + 2w_w} = \frac{2d_w w_w}{d_w + w_w} \approx 2d_w,\ w_g = w_d$$
$$or \tag{10}$$
$$D_H = \frac{4d_w w_g}{2w_g} = 2d_w,\ w_g < w_d$$

If the gate thickness controls the calculation, the perimeter is defined by the width of the gate only and the hydraulic diameter is

$$D_H = \frac{4d_g w_g}{w_g} = 4d_g \tag{11}$$

Once the appropriate thickness is specified, the hydraulic diameter is computed and the convective heat transfer coefficient is calculated using equation (9).

If the entry length condition of equation (8) is not satisfied, a correction factor can be applied to the Nusselt number to improve the result,

$$Nu_{d-adj} = Nu_D * 1.72 * \left(\frac{D_H}{x_{f_s}}\right)^{0.16} \tag{12}$$

The adjusted Nusselt number should be used to compute the heat transfer coefficient in such cases. If the Peclet number condition does not apply, an extremely rare situation for high pressure die casting, the solution for the convective heat transfer coefficient does not apply.

Surface Heat Transfer Coefficient

The surface heat transfer coefficient is the primary empirical parameter in the entire fill time formulation. It is also the most difficult to find in the literature or determine empirically. Recall that for the fill time calculation only the very short period of time after the metal reaches the gate is of interest. Much of the work reported in the literature includes both the filling period and post fill cooling which may confound the results. Work that back calculates an overall heat transfer coefficient is sensitive to data acquisition issues, assumptions made to make the problem tractable, and difficulties with inverse calculations that may be needed to determine die surface temperatures and/or metal temperatures. The very short fill times in addition to these problems combine to make the problem of finding reliable surface heat transfer coefficients difficult.

Nelson (Nelson 1970) reported a value of about 65,000 W/m^2 ^{o}K based on methods that incorporated latent heat and to this day appears to be the best estimate of this coefficient. This value has worked well in application of these results.

Time-Varying Fast Shot Profiles

The heat transfer coefficient defined via equations (7) and (9) exhibits very significant change with speed and thickness. The dependence is shown in Figure 5. It is clear from the figure that the coefficient is smallest at slow speed and large hydraulic diameters (thickness). Also, sensitivity to speed is maximized at larger thicknesses and sensitivity to thickness is maximized at slower speeds. This pattern suggests that a shot profile in which slow speeds are used throughout the period that the runner is filled and through initial thicker sections, assuming the gating is such that thin sections are filled from thick, followed by faster speeds to complete cavity fill might be feasible since heat loss will be less during the initial stages than if a faster speed was used and the higher heat loss associated with faster speeds is limited to a short period of time.

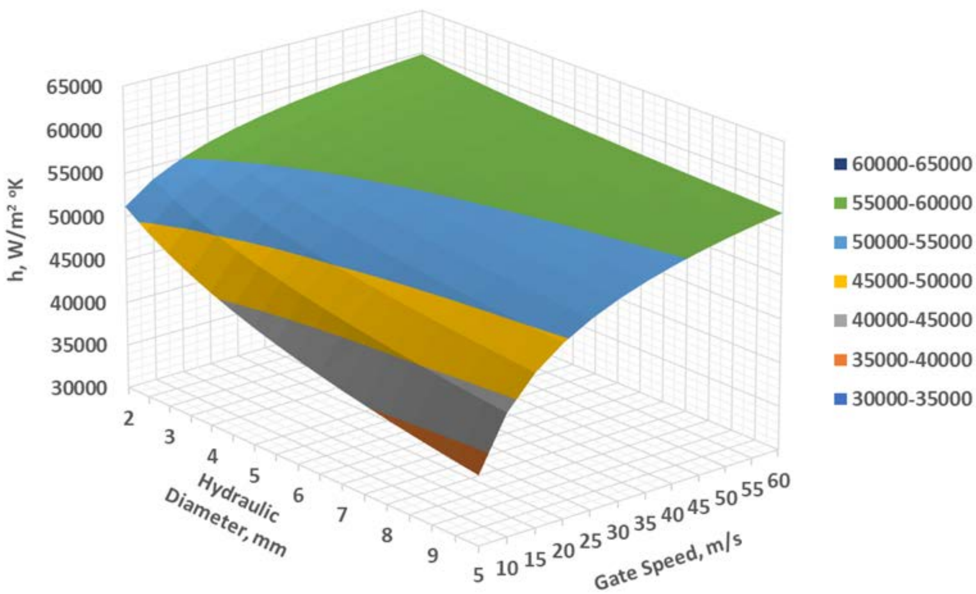

Figure 5 Heat Transfer Coefficient Dependence on Speed and Hydraulic Diameter

Equation (25) in the appendix is the solution of the differential equation that describes the time-varying case. The form of the solution shows that the temperature drop depends on the time average of a coefficient that depends on the heat transfer coefficient, hydraulic diameter of the channel and alloy properties. The fill time of the cavity depends only on the average speed. Since fill time and temperature drop depend on different averages, a time-varying shot profile can in some situations result in a lower temperature drop and more fluid metal at the end of fill compared to a constant speed profile with the same fill time. This result supports and partially explains practical experience that partial prefilling of the cavity, in some instances, produces better casting. Details and simulation examples showing the advantages of prefill in reducing air pressure in the cavity and improving venting can be found in (Miller and Monroe 2017).

Results and Discussion

The model established by Equation (2) and related equations estimates the time available before metal entering the cavity cools to the point that the fraction solid equals the user specified input. Equation (3) establishes the distance that the metal flows before this condition is reached. Each of these quantities, flow time and flow distance, is a fluidity measure. Equation (4) is perhaps the most important result that provides the gate area needed to fill the cavity under the specified conditions.

The model ties together part geometry, through the wall thickness, gate speed, and various material properties. In addition to the use for gate selection, the model can be used to examine the relative contribution of each factor to the fluidity of the alloy and the ability to fill a thin wall casting.

Sensitivity Study – Aluminum Based

The sensitivity studies are run using the model described by Equations (2) and (3). The first study is roughly based on the properties of aluminum alloys although it is important to note that no specific alloy is modeled. The first analysis uses ten factors with two levels each as listed in Table 2. The factor levels span or exceed levels found for aluminum alloys, and in the case of latent heat, greatly exceed the range to better extract the sensitivity of flow distance to this parameter. With the exception of latent heat, parameters that do not vary much from alloy to alloy are not included as factors in the analysis.

Table 2 Factor Definitions for Study One

Variable	Low	High
Freezing Range	50 ^oC (90 ^oF)	150 ^oC (270 ^oF)
Latent Heat of Fusion	349,600 J/kg	427,300 J/kg
Fraction Solid Curve	Low (defined next figure)	High (defined next figure)
Target Fraction Solid	0.50	0.80
Solidus Temperature	480 ^oC (896 ^oF)	565 ^oC (1017 ^oF)
Superheat	5 ^oC (9 ^oF)	55 ^oC (100 ^oF)
Die Temperature	175 ^oC (347 ^oF)	345 ^oC (653 ^oF)
Gate Speed	25.4 m/s (1000 in/s)	50.8 m/s (2000 in/s)
Surface Heat Trans. Coef.	48,750 W/m^2 ^oK	81,250 W/m^2 ^oK
Wall Thickness	1.27 mm (0.05 in)	2.54 mm (0.10 in)

The following property values are used and are held constant across all conditions:

alloy density 2740 kg/m^3

alloy thermal conductivity 96 W/m ^oK

alloy specific heat 963 J/kg ^oK

The fraction solid curves used as factors are as defined in Figure 6. The low level maintains a higher fraction solid throughout the upper end of the temperature range. The high level does the opposite with the fraction solid dropping rapidly over the upper end of the temperature range. Note that the figure is constructed using proportion of the freezing range as the X axis. Therefore, a point at 1 on this axis corresponds to the liquidus temperature and 0 to the solidus temperature. The curves are somewhat extreme by design to magnify the effect of the curves on flow distance.

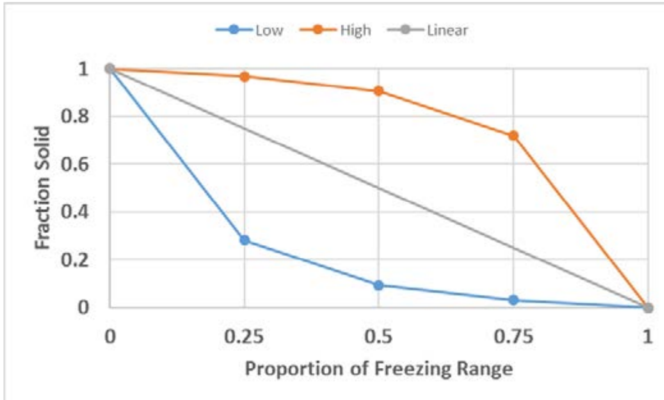

Figure 6 Fraction Solid Curve Definitions

Results – 10 Factors, 2 Levels per Factor

A Pareto plot of the 10 factor, 2 level study is shown in Figure 7. This plot shows the absolute value of the effects ordered from maximum to minimum contribution. No 3rd or higher order effects were considered in the estimation of the statistical model in this analysis so only main effects and 2nd order interactions are shown. All higher order effects are aggregated and assumed to be noise providing the basis for estimating the significance of the included effects.

The two dominant effects shown on both Figure 7 are the thickness and speed (gate speed). Each has roughly twice the effect as the other factors. As would be expected, and as can be seen from the magnitude of the HK interaction, increasing either the part wall thickness or gate speed increases flow distance.

Third on the Pareto is the target fraction solid which shows that filling to a fraction solid of 0.85 instead of 0.5, assuming that is possible, would have a little more than one half of the benefit obtained by increasing the gate speed from 25 m/s to 50 m/s. The fraction solid effect is nearly identical to the die temperature effect.

The 2-way interactions and main effects for the study are plotted in Figure 8 and Figure 9 respectively. There are small interactions that might be expected, but patterns are fairly consistent and show minimal interactions. Die temperature, speed and to a lesser degree the surface heat transfer coefficient and target fraction solid have bigger effects with thicker walls. Also, the fraction solid curve makes slightly more difference at higher speed and higher wall thickness.

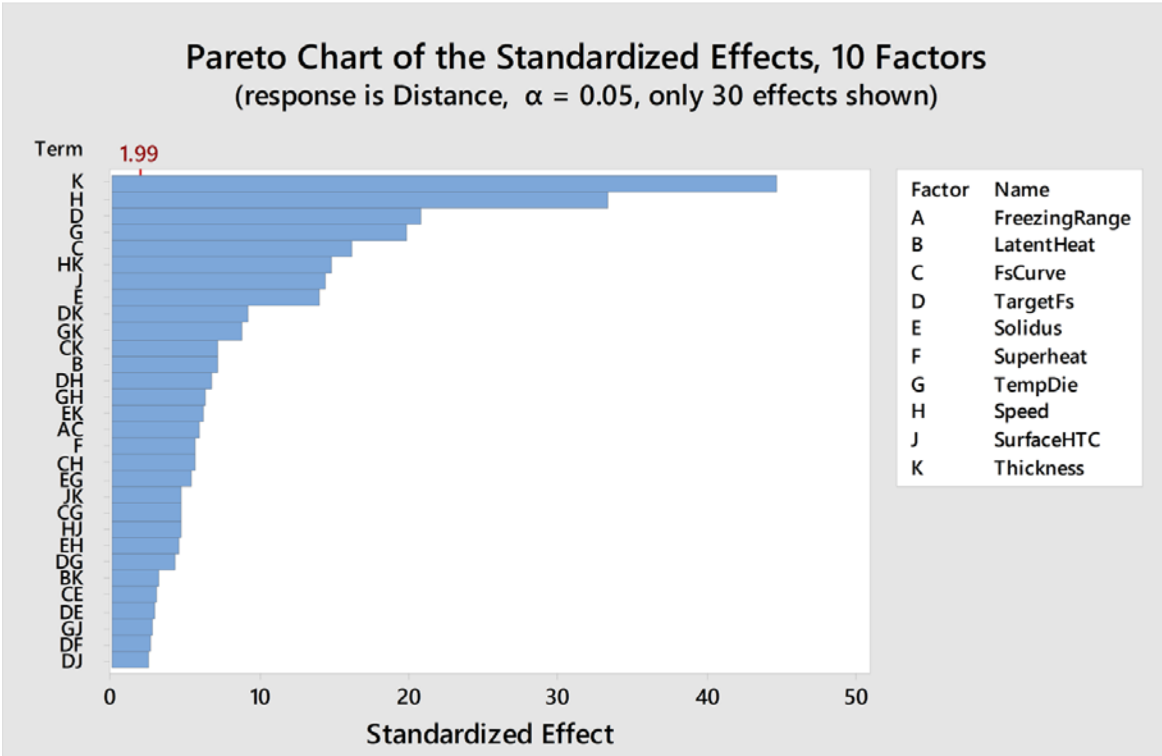

Figure 7 Pareto Chart - Study 1

More surprising than the slight interactions is the small effects from some of the factors. This is most easily seen from either Figure 8 or the main effects plot shown in Figure 9. Freezing range has very little effect, the superheat effect is small, and the latent heat effect is also small. The small freezing range effect perhaps is explained by the fact that the freezing range is most closely related to the specific or sensible heat which is small relative to the latent heat.

The small latent heat effect compared to the other factors is interesting in the sense that it is difficult to significantly change the latent heat within an alloy family and the levels used in this computational experiment are perhaps unrealistically large. Differences of even this unrealistically high magnitude are still small compared to several of the other factors.

Similar analyses were performed based on the properties of zinc alloys with similar results. Details are reported in (Miller 2016).

Note that the shape of the fraction solid curve is the materials-based factor that has the largest effect on fluidity. Note also that the magnitude of this effect is less that one half of that of speed and thickness. The target fraction solid (D) has a significant effect, but this factor is primarily a quality driven selection and not a material factor. The result does show, as is intuitively expected, that materials that flow at higher fractions solid have better fluidity as measured by flow distance.

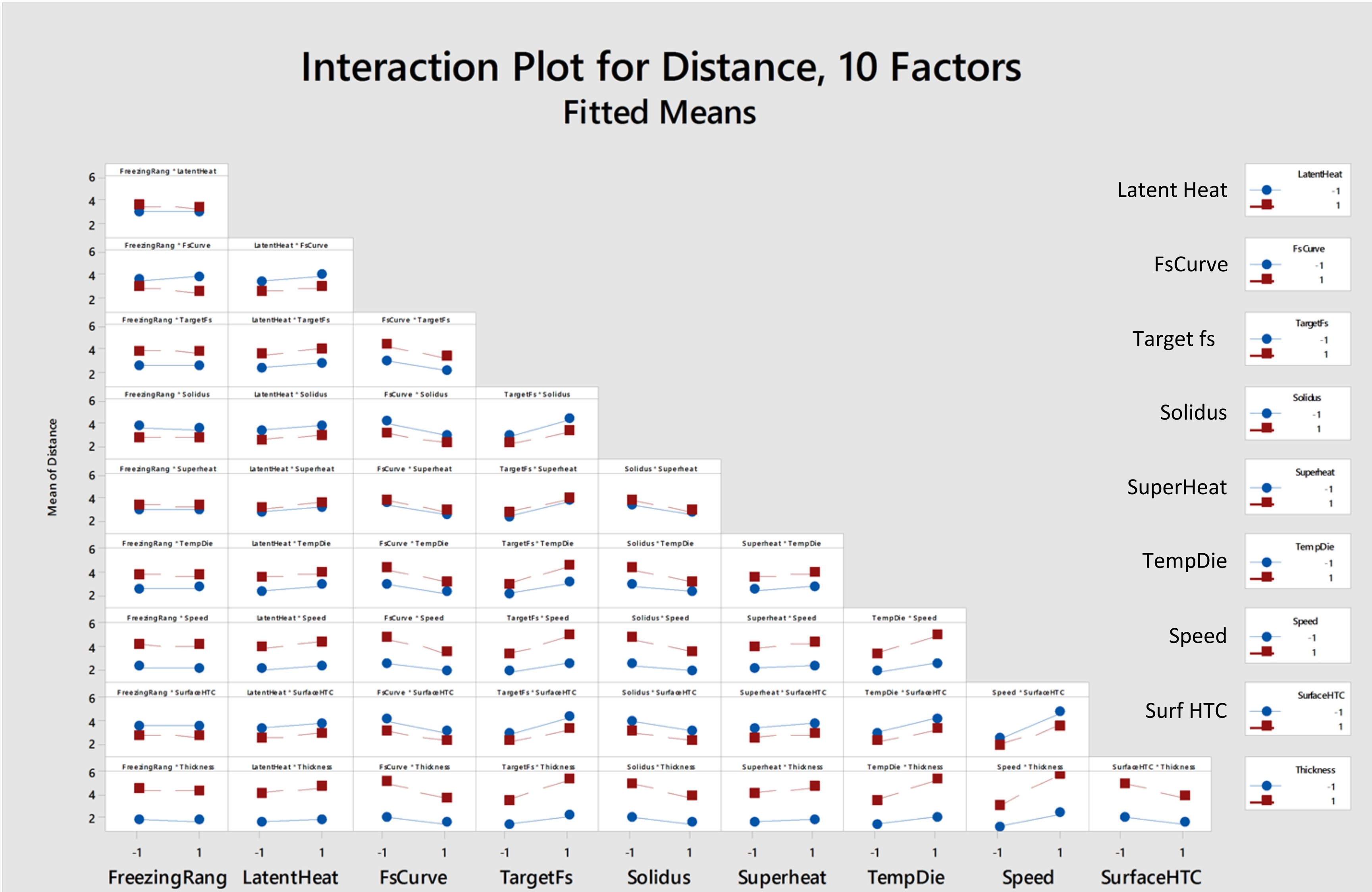

Figure 8 2-way Interactions, Study – 1

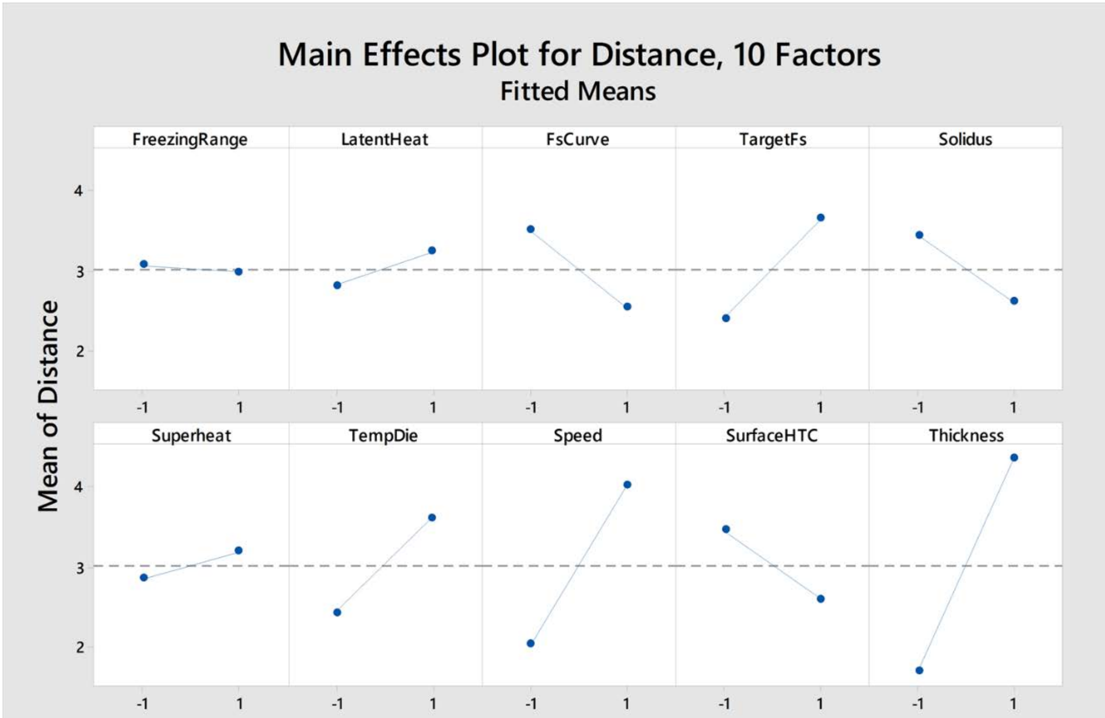

Figure 9 Main Effects - Study 1

Stoppage of Flow

From a practical point of view, the model parameter that carries the biggest uncertainty is the target fraction solid. Conventional fluidity studies that are designed to rank alloys do no provide much guidance in this regard since the processing conditions of high pressure die castings are very different from gravity and other slow fill processes.

Fluidity has been widely studied in the literature and a good overall summary is provided by Campbell (Campbell 2003). Campbell describes the conditions under which flow stops as follows:

> "The stream develops as a slurry of dendritic crystals. … when the amount of solid in suspension exceeds a critical percentage, the dendrites start to interlock, making the mixture unflowable."[1]

The idea is illustrated by Figure 10, also adapted from Campbell[1]. The argument is that when the dendrites become sufficiently tangled, flow is blocked, but the question is; How tangled is tangled?

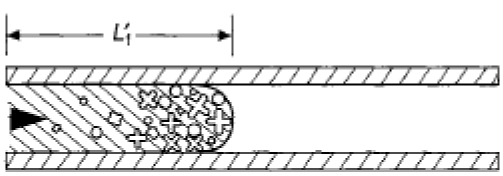

Figure 10 Flow Arrest by Partial Solidification (from[1])

[1] Campbell, J. (2003). Castings. Burlington, MA, Elsevier Butterworh-Heinemann.Chapter 3, Page 75

An expression for flow length, due to Flemings and reported by (Campbell 2003), is

$$x_f = f \cdot v \cdot t_{freeze};\ 0.2 \le f \le 0.5 \tag{13}$$

where v is the speed of the metal, t_{freeze} is the solidification time and x_f is the flow length. There is a similarity to Equation (3) except that (13) computes the flow length from an independently computed freezing time and then adjusts the resulting distance by a fraction solid term that accounts for alloy characteristics. The freezing time is often computed using Chvorinov's rule but that rule is applicable to mold controlled heat transfer conditions that are closer to post fill cooling than high speed fill (Dantzig and C. L. Tucker 2001).

Flow length results of Han (Han and Xu 2005)

This observation that flow distance increases under die casting conditions was confirmed by Han (Han and Xu 2005) who used a spiral fluidity die and measured flow distance under die casting conditions. The tests were run with several aluminum alloys plus pure aluminum. The gate speed was not reported but plunger speed during fast shot for all tests was 25 m/s. The die was preheated to 130 ^{o}C.

Flow lengths were compared using die casting tests and Ragone tests (Ragone, Adams et al. 1956). The Ragone results were consistent with standard solidification theory (i.e. the theory described by Campbell and summarized above). The die casting results were the opposite with longer flow lengths for the alloys. Han concluded that the best predictor of flow length was the solidus temperature of the alloy, the lower the solidus temperature, the longer the flow distance.

Han's results are consistent with the predictions of the model presented here. Han did not vary gate speed or die temperature and looked only at the alloy properties. The test was designed to allow the metal to flow as far as possible so the target fraction, while not possible to quantify, was simply as large as possible. The actual differences in fraction solid curves for the alloys tested are not available so it is not possible to judge how much the curves contributed to Han's results. Figure 9, the main effects plot for the aluminum sensitivity study, also shows that the solidus temperature is the most significant of the material factors aside from the fraction solid curve factors.. Han's conclusion that alloys can flow at high fractions solid qualitatively support the use of higher target fraction solid values compared to values that have been previously reported.

A few preliminary thoughts on why die casting supports longer flow distance are presented in the next two sections.

Kinetic Energy Considerations

This general depiction of flow stoppage and the range of fraction solid values is based on gravity casting where the speeds are low. The idea that higher speeds increase flow length can be inferred from (13) but the use of speed is ruled out due to the flow regime problems that are created by higher speeds. Flemings also observed that the flow distance seems to be related to the head of the metal filling the mold although this influence is only indirectly accounted for through the velocity term.

The range of values suggested for the fraction solid multiplier is sometimes cited as the applicable limit for high pressure die casting. This is a dubious extension of the gravity casting result. Table 3 contains a summary of the total heat and kinetic energy per gram for aluminum and zinc alloys. The kinetic energy values are computed for a range of speeds including approximate gravity casting speeds (0.25 m/s) and the upper end of typical high pressure die casting speeds. Table 4 presents the ratio of the total heat entry to the kinetic energy entry for the listed speeds. Kinetic energy is a negligible proportion of the total energy at gravity casting speeds (0.2% for zinc and an order of magnitude less for aluminum). The situation is reversed for die casting speeds, particularly at the higher speeds where kinetic energy is more than 4 orders of magnitude higher than heat energy.

Table 3 Heat vs Kinetic Energy for Various Conditions

	Latent +	Kinetic Energy at Speed			
	Sensible Heat	**0.25 m/s**	**1 m/s**	**25 m/s**	**50 m/s**
Aluminum	485 J/g	0.09 J/g	1.4 J/g	856 J/g	3425 J/g
Zinc	112 J/g	0.2 J/g	3.3 J/g	2063 J/g	8250 J/g

Table 4 Ratio of Kinetic Energy to Heat, Various Conditions

	Speed			
	0.25 m/s	**1 m/s**	**25 m/s**	**50 m/s**
Aluminum	0.0002	0.003	1.8	7.1
Zinc	0.002	0.03	18.4	73.6

The significance of this difference in kinetic energy is that while flow might be blocked at low fractions solid at gravity casting speeds, the high level of kinetic energy will likely carry die cast material father down the channel. In other words, the die cast material will flow farther than the gravity cast material simply due to much, much higher kinetic energy and inertial forces. The fraction solid range of 0.2 to 0.5 is likely to be too low for high pressure die castings.

Reynolds Number and Navier-Stokes

Another way of looking at the stoppage issue is to look at the flow conditions and how they change as heat is lost from the moving metal. The Navier-Stokes equation describes the flow of viscous materials. In dimensionless form, the equation includes the Reynolds number, which is the ratio of inertial forces to viscous forces, and the Froude number, which is the ratio of inertia forces to gravity. When the Reynolds number is large, flow is dominated by inertia and viscous forces are insignificant. When the Froude number is large, gravity is insignificant. The two numbers are defined as follows:

$$\mathrm{Re} = \frac{\rho \cdot v \cdot D_H}{\mu}; \qquad Fr = \frac{v^2}{g \cdot D_H} \tag{14}$$

where ρ denotes density, v speed, D_H hydraulic diameter, μ viscosity, g acceleration due to gravity. The Reynolds and Froude numbers are shown in Table 5 based on a 2 mm hydraulic diameter, density 2680 kg/m3 and viscosity 0.015 Pa-s. The viscosity is approximately that of the aluminum 319 alloy at about 650 ^{o}C or about 40 ^{o}C of superheat. The fraction solid is 0 at this temperature and the conditions are approximately those that might apply at the start of injection.

Table 5 Reynolds and Froude Numbers at the Gate

	Speed			
	0.25 m/s	**2.5 m/s**	**25 m/s**	**50 m/s**
Re at 650 °C, f_s = 0	89	893	8,933	17,867
Fr at at 650 °C, f_s = 0	3.2	319	31,888	127,551

The magnitude of the Reynolds numbers suggests that viscosity is relatively insignificant for any of the speeds listed at the given temperature. The Froude number, however, shows that gravity is important at the 0.25 m/s which is not surprising since this is approximately the speed of the metal in gravity casting. Note also that the Reynolds number is two orders of magnitude larger than the gravity casting speed at 25 m/s, near the lower end of die casting speeds, and even more at 50 m/s.

Viscosity of the metal increases as the fraction solid increases as shown in Figure 11 that displays such data for 319 and 356 aluminum alloys. 319 is used for this illustration that follows. These data were used because data for conventional die casting alloys were not available. It is clear from Equation (14) that Reynolds number depends on the viscosity and will decrease as the viscosity increases. These facts can be used to estimate the viscosity at which the inertial forces are no longer dominant and Figure 11 can then be used to estimate the fraction solid at which this occurs. The estimated fractions solid of the 319 alloy at which Re=10 and Re=1 are shown in Table 6.

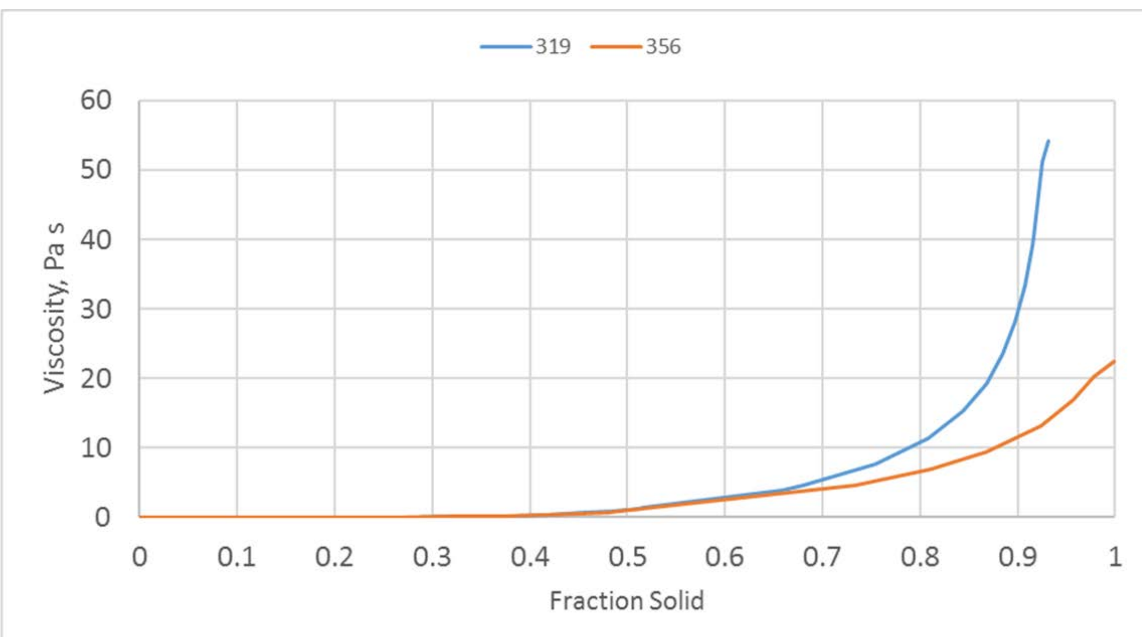

Figure 11 Viscosity as a Function of Fraction Solid, Aluminum 319 and 356 Alloys

Table 6 Fraction Solid and Reynolds Number by Speed

	Speed			
	0.25 m/s	**2.5 m/s**	**25 m/s**	**50 m/s**
f_s at which Re = 10	0.33	0.52	0.82	0.89
f_s at which Re = 1	0.52	0.82	0.89	>0.93

The range of fractions solid estimates for gravity casting speeds are in line with Fleming's range. The 2.5 m/s values are similar to those cited for squeeze and semi solid casting and while Han did not make a quantitative statement about the fraction solid range, he did point out that it should be above 0.5 as is the case with these estimates. It must be noted, however, that these estimates are based on a 2 mm hydraulic diameter and the estimates would be larger for thicker walls. A second factor is that the calculations are based on the initial gate speeds which would be lower inside the cavity due to turbulence and energy losses as the flow progresses. In general, estimates computed this way will be optimistic.

In summary, both kinetic energy and fluid flow properties at die casting conditions point to the ability to support flow at high fractions solid. The sensitivity analyses performed earlier show that flow distance can be increased by taking advantage of this property.

Conclusions

Model and Model Development

Basic principles of thermodynamics and heat transfer were used to derive a model for the maximum flow distance and maximum fill time before the leading edge of the fill front reaches a specified fraction solid. These results replace the standard "Gating Equation" that has been taught by NADCA as a tool for use with PQ^2 analysis and sizing gates for over 40 years. Key advantages of the new result are:

1) Only standard material properties are used,
2) The results are based on accepted engineering principles of heat transfer,
3) Application of the results is easily extended to new alloy systems and
4) Over estimates of fill time and physically impossible fill times are eliminated.

This work better integrates the fill time/fill distance calculation with gate area selection and perhaps helps to focus the analysis on the question of the gate area.

It is extremely important to remember that the maximum fill time calculation is not necessarily a prediction of the fill time that will be observed in operation by inspection of a shot trace. The purpose of the maximum fill time estimate is to obtain a gate area consistent with the minimum gate speed constraint and a fraction solid limit. Actual operation should be at an interior point of the window which means that the operating gate speed will be higher than the minimum and the actual fill time will be less than the calculated maximum. The measured fill time when operation is more or less in the center of the operating window should be less than the calculated maximum.

Published target fractions solid design values in older NADCA literature are probably low and should not be used without care in this model. A qualitative, macroscopic analysis was performed to provide some credibility to larger fraction solid values than have been historically used, but it is an open question as to whether or not the guidance about target fraction solid has a solid scientific basis. This is an area in need of additional work.

A key advantage of the new results is the elimination of non-standard empirical constants that limited the applicability of the older model. The only empirical parameter in the new equations is the surface heat transfer coefficient but experience has shown that existing data provide a reasonable default for this parameter.

Technology Transfer and Implementation

This model has been implemented and fully integrated in three web-based applications available on the NADCA Members Plus website. The three applications are:

4) PQ^2
5) Max Flow Time Estimator
6) Gate Designer

The PQ^2 application is used to properly size the in gate to the cavity to meet part quality requirements and to maximize the size of the operating window of the process.

The second of these applications estimates pre-injection heat losses, i.e. losses during ladling, pouring and residence of the metal in the cold chamber prior to injection. This set of calculations replaces a difficult to estimate quantity, the temperature of the metal at the gate, with estimates based on more easily obtained data.

The gate designer application is primarily intended for constructing gate geometries that facilitate metal flow into the cavity but the gate area calculation is included so that users who do not perform a PQ^2 analysis first have access to the result.

The course presentations and text materials used for PQ^2 and Gating have been revised to include the new results. The revised materials have been used for courses taught numerous times starting with the second quarter of 2016

Material and Process Sensitivity Analyses

Sensitivity analyses were performed to determine the relative contributions of process parameters such as die temperature, melt superheat at injection, and gate speed. Material parameters such as specific heat, freezing range, solidus temperature, target fraction solid or the fraction solid at which flow terminates, and the shape of the fraction solid versus temperature curve were considered. The effect of the wall thickness was also considered. The results showed that thickness is the factor with the largest impact on flow distance. If thickness is set to the low level and removed as a factor, speed, die temperature and the target fraction solid have the largest influence. Lower solidus temperatures also increase flow distance, but the effect is considerably smaller than the other factors mentioned above. Freezing range and superheat make relatively weak contributions. As a generalization, it can be said that process variables have the biggest influence, but alloys that flow at higher fractions solid compared to other members of the alloy family will have better fluidity. Extra speed or higher die temperatures will improve flow distance, but die life and similar issues must also be considered.

Based on these sensitivity studies, in order of importance to increasing flow distance, actions that will increase flow distance are as follows:

1. Maximize the wall thickness
2. Maximize the gate speed
3. Use higher die surface temperature
4. Use an alloy that flows at higher f_s
5. Use an alloy with fraction solid curve with flat slope near liquidus
6. Use a more insulating die surface, i.e. surface with lower surface heat transfer coefficient
7. Use an alloy with a lower solidus temperature

A comparison of the relative magnitude of kinetic energy to heat was used to show that castings made at die casting speeds are dominated by kinetic energy. Heat dominates castings at speeds controlled by gravity, but the ratio of kinetic energy to heat is four orders of magnitude larger for die casting compared to sand casting.

A dimensionless analysis was used to estimate the fraction solid that would result in sufficient increase in viscosity to reduce the Reynolds number of the flow to the point that viscous forces would be significant. The results of this analysis for gravity casting speeds are in general agreement with the literature. The results for die casting speeds are much higher, but consistent with the one study, (Han and Xu 2005), that has empirically measured fluidity under die casting conditions. Due to the high injection speeds, inertial forces dominate and are sufficient to continue to push material long after gravity flows would be stopped.

Acknowledgements

This work was sponsored by AMC's *Casting Solutions for Readiness Program*. that is sponsored by the Defense Supply Center Philadelphia, Philadelphia, PA and the Defense Logistics Agency, Ft. Belvoir, VA.

The support of the Defense Logistics Agency and of the NADCA Computer Modeling Task Group is gratefully acknowledged.

In addition, the author extends sincere thanks to Alex Monroe of Mercury Marine for his many comments, suggestions, supplying the production data used for verification, and particularly for his interest in this work. His insights have been most helpful.

References

Campbell, J. (2003). Castings. Burlington, MA, Elsevier Butterworh-Heinemann.

Dantzig, J. A. and I. C. L. Tucker (2001). Modeling in Materials Processing. Cambridge, UK, Cambridge University Press.

Dantzig, J. A. and M. Rappaz (2009). Solidification. Boca Raton, FL 33487, CRC Press, Taylor and Francis Group.

Han, Q. and H. Xu (2005). "Fluidity of alloys under high pressure die casting conditions." Scripta Materialia **53**(1): 7-10.

Herman, E. A. (1996). Gating Die Casting Dies, North American Die Casting Association.

Kakac, S., R. K. Shah and W. Aung, Eds. (1987). Handbook of Single-Phase Convective Heat Transfer. New York, John Wiley & Sons.

Lienhard V, J. H. and J. H. Lienhard IV (2011). A Heat Transfer Textbook. Mineola, New York, Dover Publications, Inc.

Lindsey, D. and J. F. Wallace (1968). Heat and Fluid Flow in the Die Casting Process. 5th National Die Casting Congress. Detroit, MI.

Miller, R. A. (2015). The "Gating Equation" Updated. Die Casting Congress and Exposition. Indianapolis, NADCA.

Miller, R. A. (2016). Fluidity from a Heat Transfer Perspective. 2016 Die Casting Congress and Tabletop. Columbus, OH, NADCA.

Miller, R. A. and A. K. Monroe (2017). Benefits and Limitations of Time-varying Fast Shot Profiles. 2017 Die Casting Congress & Tabletop. Atlanta, GA, NADCA.

Nelson, C. W. (1970). Nature of Heat Transfer at the Die Face. 6h SDCE International Die Casting Congress. Cleveland, OH.

Ragone, D. V., J. Adams and C. M. Taylor (1956). "A New Method for Determing the Effect of Solidification Range on Fluidity." Transaction of American Foundry Society **64**: 653-657.

Reed, C. B. (1987). Convective Heat Transfer in Liquid Metals. Handbook of Single-Phase Convective Heat Transfer. S. Kakac, R. K. Shah and W. Aung. New York, John Wiley & Sons.

Appendix: Consideration of Latent Heat using Conservation of Energy

For processes involving solidification, the change in enthalpy of the cooling casting must be equal to the heat removed in order to satisfy the conservation of energy (first law of thermodynamics) (Dantzig and C. L. Tucker 2001, Dantzig and Rappaz 2009). Specific enthalpy at temperature T is defined as

$$H(T) @ \int_0^T c_p dT + L_f \left(1 - f_s\left(T\right)\right) \tag{15}$$

where

$H(T)$	Specific Enthalpy at temperature T, J/g, (BTU/lb)
c_p	Specific heat, $J/g\ °K$, $(BTU/lb\ °F)$
L_f	Latent heat of fusion, J/g, (BTU/lb)
$f_s(T)$	Fraction solid at temperature T

Using the same framework used by (Lindsey and Wallace 1968) with the exception that enthalpy is used to account for latent heat release, conservation of energy applied a small volume of length *dx* traveling at speed v_m in a channel with wetted perimeter *P,* constant die wall temperature T_{die} and constant mass flow rate $\dot{m}$ is given by

$$\dot{m} * dH\left(T(x)\right) = q_w\left(T(x)\right)Pdx \tag{16}$$

where:

$dH(T)$	Enthalpy differential, *J/g, (BTU/lb)*
$\dot{m}$	Mass flow rate, *g/s, (lb/s)*
$T(x)$	Temperature at position *x*, *°C, (°F)*
P	Wetted perimeter of channel, *m, (in)*
$q_w(T)$	Net heat flux to/from wall, *J/s m²*, *(BTU/s in²)*
dx	Distance differential, *m, (in)*

The heat flux at the wall is proportional to the temperature difference between the casting and die,

$$q_w\left(T(x)\right) = -h\left(T\left(x\right) - T_{die}\right) \tag{17}$$

where

h	Effective heat transfer coefficient, $W/m^2\ {}^oK$, $(BTU/s\ in^2\ {}^oF)$

Combining equations (16) and (17), leads to the differential equation (18) that describes the change in enthalpy with distance traveled by the molten metal,

$$\frac{dH\left(T(x)\right)}{dx} = -\frac{hP}{\dot{m}}\left(T\left(x\right) - T_{die}\right) \tag{18}$$

From the definition of enthalpy, equation (15),

$$\frac{dH}{dx} = \frac{dH}{dT}\frac{dT}{dx} = \left(c_p - L_f\frac{df_s\left(\mathrm{T}\right)}{dT}\right)\frac{dT}{dx}$$

Combining with equation (18),

$$\left(c_p - L_f\frac{df_s\left(\mathrm{T}\right)}{dT}\right)\frac{dT(x)}{dx} = -\frac{h}{\dot{m}}P\left(T(x) - T_{die}\right),\ T\left(0\right) = T_{gate} \tag{19}$$

The first term of equation (19) requires the slope of the fraction solid curve with respect to temperature. The fraction solid curve can be quite complex and is often known only in terms of sample points that are computed using one of the commercially available thermodynamics-based material properties programs. A typical fraction solid curve is shown in Figure 12. A spline approximation to such numerical data can be used but that level of complexity is not required for basic fill time prediction. A brief summary of the solution using a general spline approximation is included in (Miller, 2015).

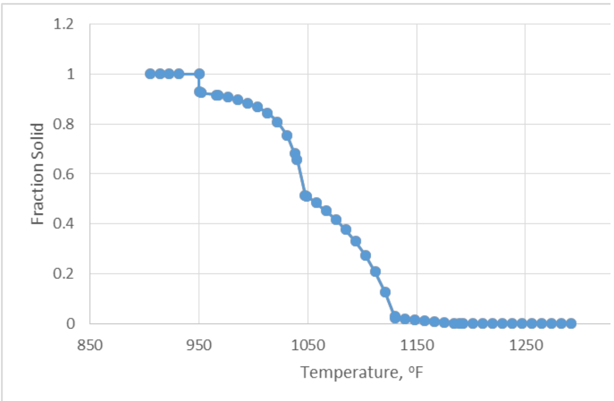

Figure 12 Typical Fraction Solid vs Temp. Curve

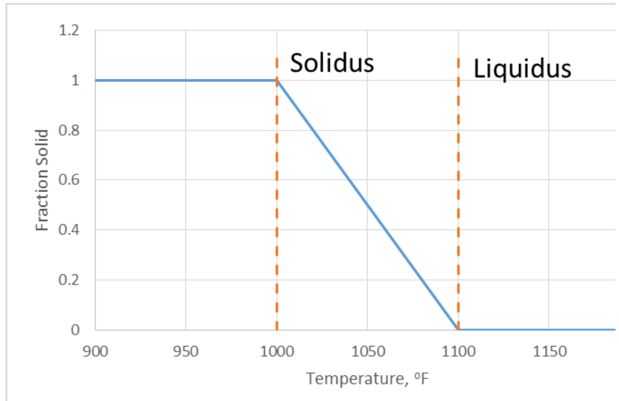

Figure 13 Typical Fraction Solid Linear Approximation

The linear approximation requires only the liquidus and solidus temperatures of the alloy,

$$f_s(T) = \begin{cases} 1, & T \le T_{solidus} \\ 1 - \dfrac{T - T_{solidus}}{T_{liquidus} - T_{solidus}}, & T_{solidus} < T \le T_{liquidus} \\ 0, & T_{liquidus} < T \end{cases} \tag{20}$$

The slope is equally simple as illustrated by Figure 13 and described in equation (21) below.

$$\frac{df_s(T)}{dT} = \begin{cases} 0, & T \le T_{solidus} \\ \dfrac{-1}{T_{liquidus} - T_{solidus}}, & T_{solidus} < T \le T_{liquidus} \\ 0, & T_{liquidus} < T \end{cases} \tag{21}$$

As expected with the linear function, and as shown by equation (21), the slope of the fraction solid curve with temperature is zero outside the freezing range and constant and non-zero within the range. This results in two different coefficients in equation (19), one that applies within the freezing range and the second that applies everywhere else.

To simplify the notation somewhat, define a multiplier $\gamma(T)$ as given below in equation (22):

$$\gamma(T) \equiv \begin{cases} 1, & T \le T_{solidus} \\ \dfrac{c_p\left(T_{liquidus} - T_{solidus}\right)}{c_p\left(T_{liquidus} - T_{solidus}\right) + L_f}, & T_{solidus} < T \le T_{liquidus} \\ 1, & T_{liquidus} < T \end{cases} \tag{22}$$

With this definition, equation (19) can be written as

$$\frac{dT(x)}{dx} = -\gamma(T)\frac{hP}{c_p\dot{m}}\left(T(x) - T_{die}\right),\ T(0) = T_{gate} \tag{23}$$

The equation can be rewritten in terms of the metal speed and the hydraulic diameter of the channel by substituting for the mass flow rate and using the definition of the hydraulic diameter resulting in the general form of the equation,

$$\frac{dT(x)}{dx} = -\gamma(T)\frac{4h}{c_p\rho v_m D_H}\left(T(x) - T_{die}\right),\ T(0) = T_{gate} \tag{24}$$

The multiplier $\gamma(T)$ is equal to 1 outside of the solidification range and is a function of the latent heat and freezing range within. The nonlinearity of equation (22) switches the coefficient of the differential equation when the temperature passes into and out of the freezing range. When the temperature is within the freezing range, the overall coefficient is reduced by the ratio of the sensible heat to the total heat (latent plus sensible) of the alloy. For many alloys, this is a significant change in the magnitude of the coefficient and accounts for the reduction in the slope of the temperature curve inside the solidification region as shown in Figure 1.

Because of the nonlinearity, equation (23) must be solved piecewise with switches to the solution occurring at the liquidus temperature and the solidus temperature resulting from the changes in the value of γ as defined by equation (22) The temperature at the end of a solution segment becomes the initial condition for the next segment. Three distinct cases are possible:

1. $T_{gate} > T_{liquidus}$, $\gamma = 1$
2. $T_{solidus} < T_{gate} \le T_{liquidus}$, $\gamma = \dfrac{c_p\left(T_{liquidus} - T_{solidus}\right)}{c_p\left(T_{liquidus} - T_{solidus}\right) + L_f}$
3. $T_{gate} \le T_{solidus}$, equation does not apply

For case 1, equation (23) is solved with $\gamma=1$ from the initial condition to the point at which the temperature reaches the liquidus. This result is then used as the initial condition to solve the equation again with γ defined by the middle condition of equation (22). This solution applies until the solidus temperature is reached. The defining equation applicable below the liquidus temperature requires a different formulation since the equation used here is based on convective heat transfer from the moving liquid metal and the die and does not apply to conduction in stationary metal.

Solution with Varying Speed and Thickness

The solution procedure for equation (24) outlined above assumes that the coefficient of the equation is piecewise constant. If the speed and/or thickness are varying as is the case if prefill of the cavity is used, the coefficient is time-varying and the solution is more complex. The solution has an exponential form but the exponent of the exponential is time varying as shown in (25).

$$T(t) - T_{die} = \left(T_{gate} - T_{die}\right) \cdot e^{-\int_0^t \left[\gamma(s) \cdot \frac{4 \cdot h(s)}{c_p \cdot \rho \cdot D_H(s)}\right] \cdot ds} \tag{25}$$

The exponent in equation (25) is the average of the coefficient over the time interval of interest. Consequently, the temperature drop in the metal will depend on the exact pattern of speed and thickness changes.